Molecular Crystals and Liquid Crystals
Publication details, including instructions for authors and subscription information:
http://www.tandfonline.com/loi/gmcl16

Photoconduction in Single Crystals of the Thianthrene-Tetracyanobenzene 1:1 Adduct

Andrzej Miniewicz [a] , Marek Samoc [a] & Digby F. Williams [b]

[a] Institute of Organic and Physical Chemistry, Technical University of Wroclaw, 50-370, Wroclaw, Poland

[b] National Research Council Canada, Division of Chemistry, Ottawa, Canada, K1A OR6

Version of record first published: 20 Apr 2011.

To cite this article: Andrzej Miniewicz , Marek Samoc & Digby F. Williams (1984): Photoconduction in Single Crystals of the Thianthrene-Tetracyanobenzene 1:1 Adduct, Molecular Crystals and Liquid Crystals, 111:3-4, 199-214

To link to this article: http://dx.doi.org/10.1080/00268948408072432

Mol. Cryst. Liq. Cryst., 1984, Vol. 111, pp. 199–214
0026-8941/84/1114–0199/$20.00/0

Printed in the United States of America

Photoconduction in Single Crystals of the Thianthrene—Tetracyanobenzene 1 : 1 Adduct

ANDRZEJ MINIEWICZ,† MAREK SAMOC† and DIGBY F. WILLIAMS

National Research Council Canada, Division of Chemistry, Ottawa, Canada K1A 0R6

(*Received March 5, 1984*)

The photoconduction of single crystal thianthrane—tetracyanobenzene has been measured as a function of excitation wavelength, 200–600 mm, excitation intensity, temperature and applied field. In the 200–325 nm region only electron photocurrents are observed which show a symbatic behaviour; in the 325–340 nm region antibatic photocurrent behavior occurs for holes and electrons; for longer wavelengths both photocurrents are weak with no wavelength dependent structure. The electron mobility was ~ 3.6 cm^2/Vs at 300 °K. These results are discussed in terms of the dominate photocarrier generation processes.

1. INTRODUCTION

The main interest in the photoconductivity of single crystals of organic semiconductors has been in the elucidation of the mechanisms of carrier generation and carrier transport. Up till now most of the experimental and theoretical work has been performed on simple one component molecular crystals, anthracene being the arch-typical material (see ref. [1] for a review). The knowledge of basic photogeneration mechanisms in these simple model materials has prepared the ground work necessary for an extension of photoconductivity studies to more complicated systems. Two-component systems, in particular

†Present address: Institute of Organic and Physical Chemistry, Technical University of Wroclaw, 50-370 Wroclaw, Poland.

the so-called charge-transfer crystals, form a very interesting class of materials for such studies, the main problems to be solved being the role of charge transfer (CT) excitons in photogeneration processes, and the applicability of photogeneration theories (such as the Onsager model).

To this end, we have undertaken a study of photoconduction in complexes of tetracyanobenzene (TCNB). Results obtained for one of the TCNB complexes, namely anthracene—TCNB have already been reported.[2] It was postulated that the main photogeneration process in this compound involves the thermal dissociation of the lowest lying CT exciton state. Our results obtained on other TCNB complexes[3] seem to confirm this point of view. Thianthrene—TCNB has, however, been found to behave differently. The present paper is concerned with rationalizing the photoconductivity spectra of thianthrene—TCNB and elucidating the photogeneration pathways in this compound. The experimental techniques employed in this study involved measurements of the steady-state photoconductivity as well as pulsed and two-photon photoconductivity.

2. EXPERIMENTAL

Single crystals of the 1 : 1 thianthrene—TCNB adduct were grown from acetone solution. The crystals were colorless (thus different from typical CT complexes of tetracyanobenzene which generally show CT absorption in the visible); dissolving them and measuring the absorption spectra in solution confirmed the 1 : 1 composition. Transparent platelets which were single crystals (checked with a polarization microscope) were chosen for the measurements. Typical sample dimensions were $3 \times 5 \times 1$ mm^3. The measurements of steady-state photoconductivity were carried out in a 'sandwich' type configuration. Photocurrent action spectra were studied using two different arrangements. The first system, used for the measurements in the spectral range 300–640 nm consisted of a 2.5 kW Xe arc coupled to a 0.75 m Chromatix grating monochromator. Crystals were mounted in a thermostated chamber and the sample temperature varied by the rate of flow of cold nitrogen gas and controlled via feedback from a thermocouple. Electrical contacts to the samples were provided by a pressure contact of conducting quartz (indium-tin oxide covered quartz slides with the resistance of 20Ω/□) and a silver paste painted electrode. The excitation light intensity was varied using a rotary neutral density filter and calibrated against a Hewlett Packard 8330A flux meter. The photocur-

rent was measured with a Keithley electrometer/chart recorder combination. To extend the measurements to 200 nm a second system was used in which the exciting light was provided by a Cary 219 spectrophotometer equipped with deuterium and tungsten-halogen lamps. Here the samples were mounted in the cell compartment of the spectrophotometer using a specially constructed sample holder with the front electrode made of quartz glass covered with vacuum deposited gold (40–50 pc transmittance). The monochromatic light intensities in this arrangement were rather low (below 3 $\mu W/cm^2$) which rendered the correcting of action spectra with respect to the spectral

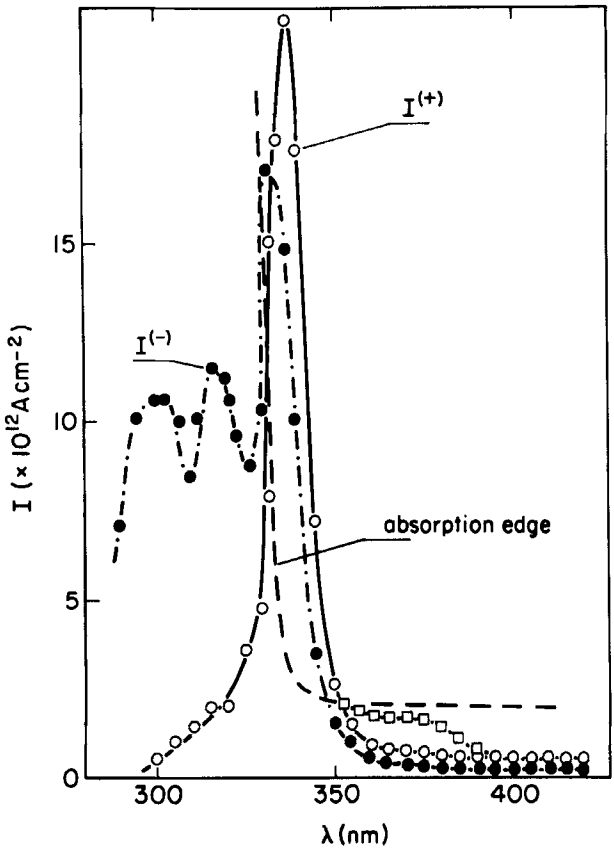

FIGURE 1 Spectral dependences of $I^{(+)}$ and $I^{(-)}$ photocurrents in thianthrene-tetracyanobenzene 1 : 1 adduct; $I^{(+)}$ and $I^{(-)}$ were corrected to $I_0 = 8 \times 10^{13}$ photons/s cm^2. The absorption edge of solid T—TCNB is marked by dotted line. Squares mark a variation in $I^{(+)}$ photocurrent action spectrum observed when a previously irradiated sample was used.

characteristics of the lamp impossible. No measurements of temperature and light intensity dependences were made in this spectral region.

The same spectrophotometer was also used for the measurements of absorption spectra of thianthrene—TCNB both in solution and in the form of crystals.

A study of two-photon induced photoconductivity was also attempted.[4] A Molectron DL-200 dye laser provided 10 ns pulses of light (up to 1.2 mJ per pulse) in the range 550–640 nm, and the photocurrent generated was integrated with a high input impedance FET follower. A double beam scope monitored the generated charge and the intensity of laser pulses.

The drift mobility of charge carriers was also determined using the well-known time-of-flight technique. The excitation source was in this case a Lumonics excimer laser working at 308 nm and supplying *ca.* 10 ns pulses.

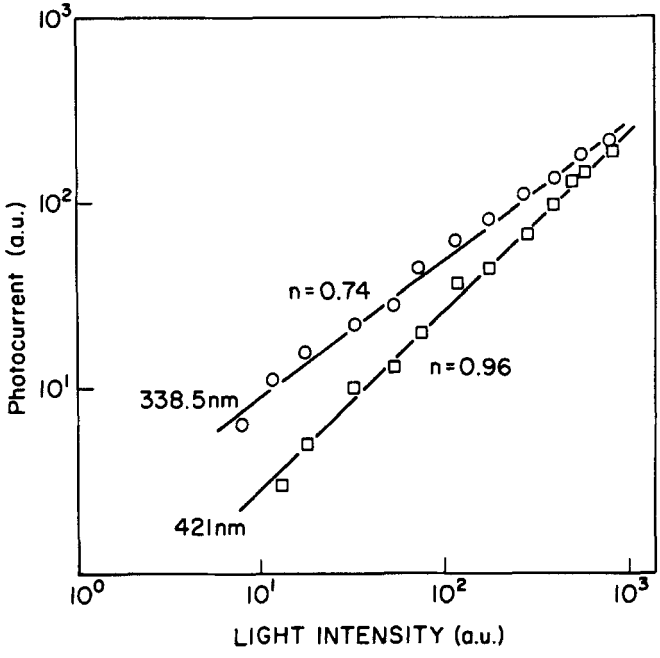

FIGURE 2 Typical light intensity dependences of the photocurrent in T—TCNB. Photon fluxes used ranged between 10^{12} and 10^{15} photons/s cm^2.

3. RESULTS

Preliminary experiments have shown that thianthrene—TCNB single crystals exhibit a strong photoresponse when irradiated with light of wavelengths shorter than ca. 340 nm (3.65 eV), however, relatively weak photocurrents could also be detected in the region 340–600 nm. Figure 1 shows typical spectral dependences of the photocurrent in a sandwich sample of thianthrene—TCBN obtained for both positively and negatively biased front electrode (we shall denote such photocurrents by $I^{(+)}$ and $I^{(-)}$, respectively) in the first experimental system.

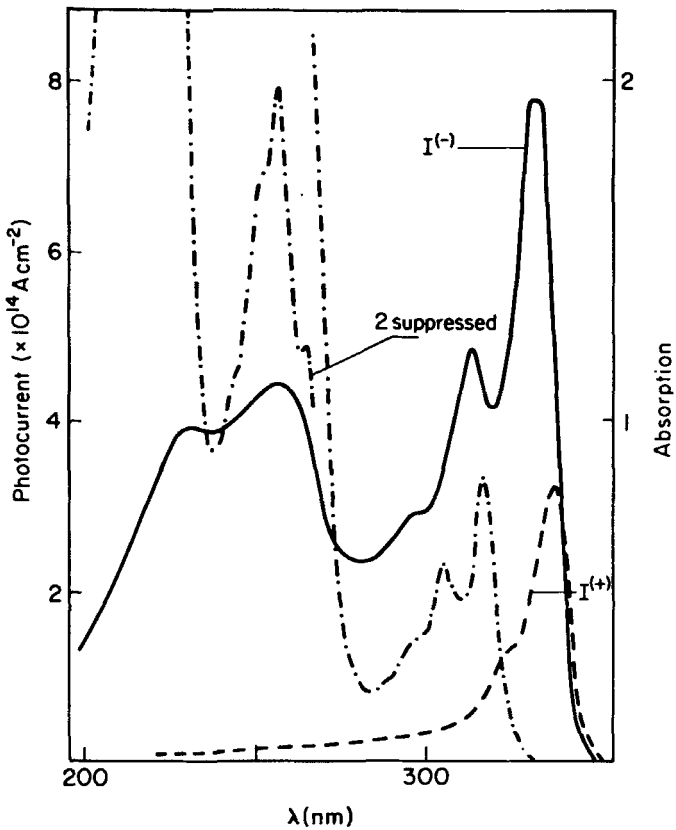

FIGURE 3 Action spectra of photoconductivity in T—TCNB in the strong absorption region uncorrected with respect to the spectral lamp characteristics (see text for details). The absorption spectrum of T—TCNB (dash-dotted line) dissolved in methanol is also presented for comparison.

The spectra were corrected by implying a linear relationship between the photocurrent and the light flux. Such a linear relationship has been found to hold for longer wavelengths, while for shorter wavelengths the light intensity dependences of the photocurrent become slightly sublinear as can be seen in Figure 2.

The peak occurring near 338 nm was found to shift towards shorter wavelengths when thinner samples were studied and the long wavelength part of the spectrum, i.e. in the region 340–500 nm was strongly sensitive to sample history, as shown in Figure 1.

As mentioned earlier the measurements of the spectral characteristics were extended to 200 nm using the Cary 219 system. The spectra, uncorrected for the wavelength variation of the light flux are presented in Figure 3, together with the absorption spectrum of thianthrene—

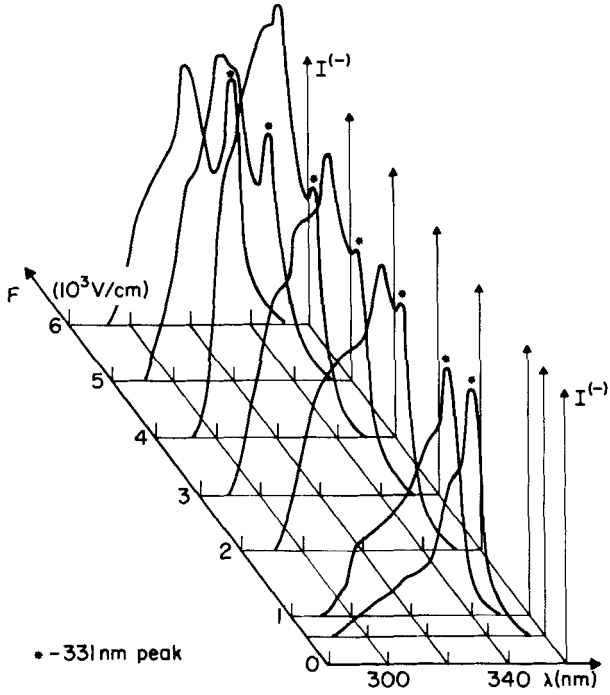

FIGURE 4 $I^{(-)}$ photocurrent action spectra versus externally applied electric field in T—TCNB. Note: the spectra have not been corrected with respect to lamp characteristic, however, they were normalized at 331 nm.

TCNB (solution). The general features of the spectra are as follows:

i) the photocurrent is strongly asymmetric with respect to the polarity of the irradiated electrode which suggests that charge carriers of only one type are mobile.

ii) the photocurrent $I^{(-)}$ shows clearly a symbatic behaviour in the strong absorption range.

Photocurrent-voltage dependences were obtained from measurements of the photocurrent action spectra (in the range 290–500 nm) with various voltages applied to the sample. It was found that the form of current-voltage characteristic depend on the wavelength of excitation. An example of this behaviour is shown in Figure 4 where $I^{(-)}$ vs. wavelength is shown for various applied voltages. In most cases the current-voltage characteristics are superlinear. A typical value of the exponent n in the relation $I \sim V^n$ which satisfies most of the measurements is ca. 1.5.

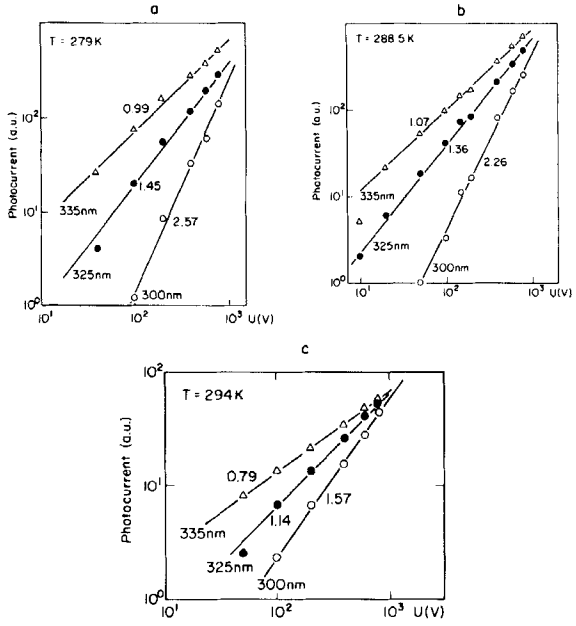

FIGURE 5 Photocurrent-voltage characteristics in T—TCNB taken at various excitation light wavelengths (300, 325 and 335 nm) and different temperatures 279 K—Figure 5a, 288.5 K—Figure 5b and 294 K—Figure 5c. Slopes of the lines are given in the figures.

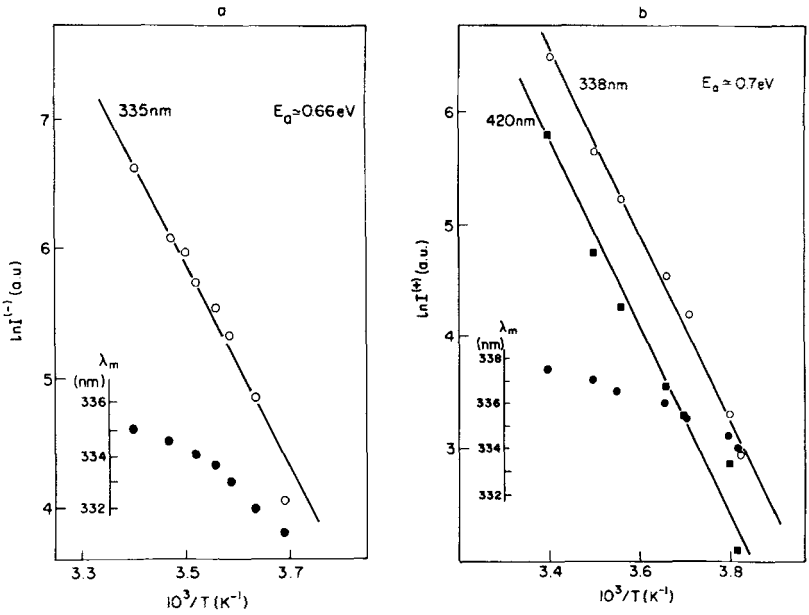

FIGURE 6 Natural logarithms of the positive (6a) and negative (6b) photocurrent (arbitrary units) versus reciprocal temperature in T—TCNB. The activation energies of photocurrents and the wavelengths of excitation light are marked in figures. The temperature shifts of the antibatic peak positions (λ_m) are plotted as inserts.

The form of the current-voltage characteristic was also found to depend on temperature. Figure 5 shows the current-voltage dependences at 279, 288.5 and 294 K. There is a tendency of n to increase with decreasing temperature and shorter wavelengths. The activation energies derived from temperature dependences of the photocurrent (Figure 6) were in the range 0.6–0.7 eV. It is interesting to note that the long wavelength peak of the action spectra exhibits a blue shift on lowering the temperature as shown in the insert of Figures 6a and 6b. It appears that these shifts may be associated with temperature changes in the long wavelength tail of the crystal absorption spectrum.

4. DISCUSSION

Before considering the possible mechanisms of photogeneration in the adduct of thianthrene and tetracyanobenzene one should note that this material cannot be considered to be a typical CT complex (as e.g.

anthracene-TCNB). Unlike other adducts of TCNB with aromatic hydrocarbons and their derivatives, there is no distinct CT band in the long wavelength part of the absorption spectrum. It is, of course, possible, that some weak CT absorption [due to donor and acceptor absorption] is buried under stronger absorption bands and its detection may be impossible by standard absorption measurements (see e.g. [5] for the detection of weak CT bands in anthracene). Nevertheless, to the first approximation, the absorption spectrum of thianthrene—TCNB seems to be a simple sum of absorption spectra of TCNB[6] and thianthrene.[7]

One can divide, somewhat arbitrarily, the photocurrent action spectrum of thianthrene—TCNB into three regions, (i) the UV region, characterized by strong absorption (*ca.* 200–325 nm) where practically no $I^{(+)}$ photocurrent is observed and the $I^{(-)}$ photocurrent shows a symbatic behaviour; (ii) the region of the Urbach tail (325–340 nm) characterized by the presence of an antibatic peak of the action spectrum, and (iii) the region of very weak absorption (340–540 nm). Photoconduction in these regions will be discussed separately.

4.1. Photoconductivity in the strong absorption range

The existence of a symbatic correlation between the photocurrent and the absorption spectrum of a solid suggest that photogeneration is an extrinsic process caused by the interaction of excitons with the surface. Indeed, since the absorption of light is complete for the sample thicknesses used, an intrinsic photocarrier generation should occur independently of the absorption coefficient, while, obviously, the efficiency of a process involving exciton diffusion towards the surface will depend on the ratio of the light penetration depth (i.e. inverse of the absorption coefficient) to the mean diffusion free path of excitons. The fact that only a negative ($I^{(-)}$) photocurrent is observed in this spectral range suggests that the photo-generation process leads to the formation of an electron at or close to the surface and that holes are either irreversibly trapped or are discharged at the electrode.

These conclusions are supported by results from attempts to measure the photocurrent induced by bulk (two-photon) creation of excitons. These experiments performed in the range 540–674 nm for light intensities of the order of 10^{23} photons/cm^2 s failed to detect a photocarrier generation which would be a two-photon analogue of the process observed in the UV range, although calculations have shown that photocurrent densities of the order of 10^{-8} Acm^{-2} could have been expected were the photogeneration process of a bulk nature.

One can thus conclude that the main contribution to the photocurrent in the strong absorption range comes from the interaction of excitons with the surface. It is, however, also possible that there are other parallel processes which play significant roles, e.g. exciton interaction with empty and/or filled charge carrier traps. The former of these processes may be of either surface or bulk type and should lead to the formation of free electrons and trapped holes (similar to crystals of phenazine[8]) whereas the latter (considered e.g. by Kalinowski and Godlewski[9] for anthracene), results in detrapping. As will be shown below, the exciton-empty charge carrier trap interaction is likely to dominate in the region of the Urbach tail.

The process of the interaction of an exciton with the surface resulting in the injection of a carrier into the sample[10-12] may be thought of in terms of the one-dimensional Onsager model. We shall discuss the problem of the quantitative description of electric field and temperature dependences of this process later. Here, however, a comment is necessary on the observed sublinearity of the light intensity dependences of the photocurrent. As shown in section 3, these sublinearities occur predominantly in the region of strong absorption. There are two possible mechanisms giving rise to this phenomenon. Firstly, one can show that the second order recombination of charge carriers should lead to sublinear light intensity dependences. It is difficult to prove whether such recombination really prevails in the experiments on thianthrene—TCNB. For a process involving excitonic injection of charge carriers (i.e. a process in which an exciton creates a charge carrier at the crystal-electrode interface and its image charge within the electrode) one should deal only with the geminate recombination of charge carriers with their image charges. Geminate recombination is obviously a first-order kinetic process and cannot lead to sublinearities in the light intensity dependences. On the other hand, exciton dissociation in the vicinity of the contact, leading to the formation of a free electron and trapped hole would provide a possibility of second order recombination of electrons and holes in the surface layer, the contribution of this process being more important for stronger absorption.

Other mechanisms which can be of importance are the interactions between excitons. As discussed in Ref. 4 thianthrene shows a very efficient channel for the creation of triplet excitons from singlet excitons via intersystem crossing. Triplets, on the other hand, undergo a second order annihilation process, leading to the formation of singlets (responsible for the delayed fluorescence of thianthrene). Although exciton interaction processes have not been studied for thianthrene—TCNB, one can assume that, similar to those in

thianthrene, the heavy atom effects of sulphur will lead to efficient formation of triplets. Therefore, for strong absorption, steady-state concentrations of singlet and triplet excitons may be expected to be complicated functions of the light intensity and the distance from the surface, since the diffusion equation governing the concentration of the excitons will contain a quadratic exciton annihilation term.

4.2. Origin of the antibatic photocurrent peak

As shown in Figures. 1 and 3, the $I^{(-)}$ and $I^{(+)}$ photocurrent spectra show long wavelength peaks at ca. 331 and 337 nm respectively, the peaks corresponding to no characteristic feature in the absorption spectrum of thianthrene—TCNB. As shown in Figure 6, the position of these peaks depends on temperature; some thickness dependence has also been noticed. The existence of such antibatic peaks is quite common in the action spectra of photoconduction in organics and many interpretations of this feature have been proposed. Generally, such peaks are due to a bulk photogeneration process which is quenched at higher values of the absorption coefficient. Thus, for the case of photoconduction in phenazine,[8] a typical condition which determines the wavelength maximum of the photoconduction action peak is that $\alpha \cdot L \approx 1$, α being the absorption coefficient and L being the sample thickness.

There is a similarity between the photocurrent action spectra reported here for thianthrene—TCNB and that observed in[8] phenazine. In both cases the antibatic peak can be observed for both polarities of the irradiated electrode while only negative photocurrent may be detected in the region of strong absorption. The interpretation adopted earlier[8] was in terms of bulk interaction of singlet excitons with defects—empty hole traps, this interaction leading to the formation of free electrons and trapped holes. A high density of recombination centres (trapped holes) thus produced would lead to the decrease of the electron photocurrent at higher values of the absorption coefficient. The appearance of an antibatic peak in anthracene—TCNB [2] has also been explained taking into account bulk recombination of charge carriers.

Clearly, this explanation is not the only one possible and to discuss the problem in detail, a knowledge of many parameters is necessary, for example, the spatial profiles of the concentrations of charge carriers of both types, the recombination coefficient, the parameters governing thermal and photo detrapping of trapped holes etc. The main conclusion which can be reached is, however, that apart from an

obviously surface controlled extrinsic photogeneration occurring in the strong absorption regime, there is also a bulk process of photogeneration in thianthrene—TCNB. Most probably it is of the exciton-defect type, since intrinsic photogeneration should give a non-zero increment to the $I^{(+)}$ photocurrent also at higher absorption coefficients which is not observed. It can be assumed that both the $I^{(-)}$ and $I^{(+)}$ photocurrents are due to the motion of electrons, the difference between them being due to the direction of motion (away from the irradiated electrode for $I^{(-)}$ and towards the electrode for $I^{(+)}$.

The temperature shifts of the positions of the antibatic peak maxima would be expected due to the sharpening of the Urbach tail of the absorption spectrum on lowering the temperature.

4.3. Photoconductivity in the region of very weak light absorption

The photocurrents observed in the region of very weak absorption (above 340 nm) were about two orders of magnitude lower than those observed in the strong absorption regime. The positive ($I^{(+)}$) photocurrent was as a rule 2–3 times larger than the negative ($I^{(-)}$) photocurrent. The magnitudes of the photocurrents depended strongly on previous irradiation history of the sample suggesting that the photocurrents may be due to detrapping of charges (probably holes). Unlike phenazine[8] no structure in the action spectrum could be observed, the currents decreased monotonically for increasing wavelength.

There are a few entities which may be active in the detrapping process. In the region 340–400 nm there is a weak absorption due to the $n\pi^*$ transition in thianthrene[4] and for longer wavelengths one should take into account formation of thianthrene and TCNB triplets (the triplet level of thianthrene is positioned near 430 nm). Since there is no spectroscopic evidence of the existence of low energy CT states in thianthrene—TCNB, the role of CT states in the detrapping processes has to be disregarded. Finally, direct interaction of photons with trapped charge carriers (i.e. absorption by ionized impurities) may also play a role.

4.4. Temperature and electric field dependences of photocurrents in thianthrene—TCNB

The electric field and temperature dependences of the photocurrents observed require some consideration. Also some comments are also necessary on the relation between the dependences of the photogeneration yield on temperature, the electric field and the properties of the photocurrent. Clearly, one cannot automatically interpret the electric

field dependences of the photocurrent as reflecting the field dependence of the photogeneration process. This is especially true when dealing with photogeneration processes occurring in the sample surface region where, first of all, space charge effects may lead to serious modification of the electric field as compared to the mean value V/L. Furthermore, trapping and recombination of charge carriers modify to a large extent the gain of the photocurrent. Some confidence in the assumption of the unity gain case (i.e. the case when all the generated charge carriers reach the counter electrode and contribute to the current) may be given by the measured mobility of electrons in thianthrene—TCNB. A time-of-flight experiment performed at room temperature using an excimer laser working at 308 nm yielded the mobility of electrons $\mu_e = 3.9\ \mathrm{cm}^2/\mathrm{Vs}$. These results indicate that bulk trapping of electrons was minimal in these samples. No hole transients could be observed, in agreement with the results of the steady-state photoconductivity.

Though it is over ambitious to offer a quantitative explanation of the observed phenomena, some qualitative features can be proposed. As discussed in the preceding subsections, the two main photogeneration processes are the interaction of excitons with the surface and the interaction of excitons with bulk traps. In both processes one can expect that the crucial step of photogeneration is the field enhanced dissociation of the geminate pair. In the former process the geminate pair consists of an electron and its image charge within the adjacent electrode, and in the latter process the geminate pair consists of a free electron and a trapped hole. The efficiency of the photogeneration process will be dependent on product of the efficiency of formation of a geminate pair (possibly field dependent) and the probability that the electron escapes recombination with its counter charge.

The most popular approach to the problem of escaping carrier recombination is couched in terms of the Onsager model which consists in solving the Smoluchowski equation of diffusion of the carrier in the electric field which is the sum of the external field and that due to the counter charge. Clearly, while the bulk process, assumed here to prevail in the weak absorption range, should be described by the three-dimensional Onsager model, the surface process could be interpreted in terms of a one-dimensional Onsager model. Charlé and Willig[13] solved the problem of a surface injection of carriers by assuming a finite rate of surface geminate recombination k_{rec}. The equation they derived for the photocurrent may be presented in the form:

$$j = b\frac{k_{\mathrm{es}}}{k_{\mathrm{es}} + k_{\mathrm{rec}}} + j_{\mathrm{ISL}}\frac{k_{\mathrm{rec}}}{k_{\mathrm{es}} + k_{\mathrm{rec}}} \tag{1}$$

where b is a constant, k_{es} is the escape velocity and j_{ISL} is the current which should flow in the ideal sink limit (considered in earlier approaches to the 1-D Onsager model[14,15]). In the case of strong light absorption and surface generation only, the first term in Eq. (1) dominates. The recombination velocity should be only weakly dependent on temperature and the electric field as it is controlled by collisions, whereas k_{es}, given by:

$$k_{es} = \frac{D \exp(e\phi(x_0)/kT)}{\int_{x_0}^{\infty} \exp(e\phi(x)/kT)\, dx} \tag{2}$$

where x_0 is the initial distance of an electron from the surface and D is the diffusion constant, should be strongly field dependent. $\phi(x)$ is the electrical potential given by

$$e\phi(x) = \frac{e^2}{16\epsilon\epsilon_0 x} - eFx \tag{3}$$

ϵ being the relative dielectric permittivity and F being the applied electric field.

In order to evaluate field and temperature dependences of k_{es} one can perform a series of calculations based on formula (2). It follows that the magnitude of k_{es} depends strongly on the assumed initial separation x_0 while the form of its field dependence is relatively insensitive to changes of x_0 in the range 0.3–1 nm. Temperature dependences of k_{es} are generally determined by the value of x_0. Temperature changes also slightly influence the form of the field dependences, however, close to room temperature, and in the range of electric fields 10^3–10^5 V/cm, k_{es} follows a power dependence $k_{es} \sim F^n$ where n lies in the range 2–2.5.

It can be seen from formula (1) that for $k_{es} \ll k_{rec}$, $j \sim k_{es}$, thus, the experimental dependences at lower temperatures and for strong absorption (see Figure 6) may be explained as arising from fulfilling this criterion. The lowering of the exponent in the photocurrent-electric field dependence on rising the temperature may be attributed to the breakdown of this approximation when k_{es} rises.

A qualitatively different situation is expected for the weak absorption regime where a bulk process dominates. The probability of escaping recombination in the bulk by three dimensional diffusion is

given by a simple formula e.g.[16]:

$$\Omega = \Omega_0\left(1 + \frac{e^3}{8\pi\epsilon\epsilon_0 k^2 T^2}F\right) \tag{4}$$

applicable for moderate field strengths. Ω_0 is here the zero field dissociation probability, given in the original Onsager model by

$$\Omega_0 = \exp\left(e^2/4\pi\epsilon\epsilon_0 kTr_0\right) \tag{5}$$

where r_0 is the initial separation of the geminate pair in the bulk. Equation (4) predicts a sublinear field dependence of the photogeneration yield which is in disagreement with the experimental results. One should, however, take into account that in both cases, i.e. both for surface and bulk photogeneration, the formation of geminate pairs may itself be field dependent and that other processes such as secondary recombination and space charge effects may contribute to the overall field dependence of the photocurrent. Nevertheless, a general conclusion is that one should expect a stronger field dependence in the surface generation spectral range and a weaker field dependence in the bulk photogeneration range. This is indeed observed in the form of the electric field dependence of the photocurrent action spectra (Figure 4). The buildup of symbatic peaks for the increase of the electric field is in agreement with the above conclusion.

One more comment is necessary on relatively large values of the activation energies of the photocurrent. It must be realized that, in terms of the Onsager model, the activation energy of ca. 0.6 eV would correspond to the initial separation of the order of below 1 nm (the exact value of the initial separation will depend on the dielectric permittivity and on the dimensionality of the process—i.e. whether one deals with one dimensional injection of carriers or three dimensional bulk process). As discussed earlier[2] such small initial separations do not necessarily lead to very low photogeneration efficiencies provided that the lifetime of the initial pair of charge carriers is large (or in other words that the recombination velocity is low). It is interesting to note that no substantial variations of the activation energy with the wavelength were observed. This is in agreement with the assumption that electronically and vibrationally relaxed excitons take part in the photogeneration processes, i.e. the excess energy of the excited states is dispersed before the excitons reach a generation site: the surface or a defect molecule.

5. CONCLUSIONS

Results presented in this paper indicate that, unlike anthracene—TCNB,[2] thianthrene—TCNB exhibits photoconduction dominated by extrinsic processes i.e. interaction of excitons with the surface, bulk defects and trapped charge carriers. This difference is probably due to the absence of a typical CT excitonic level in thianthrene—TCNB. It is possible that some intrinsic photogeneration may occur in this compound but may be buried under much stronger photoconductivity peaks due to the extrinsic processes. Changes of the photoconductivity spectra with the applied electric field may be qualitatively interpreted on the basis of the generalized 1-dimensional Onsager model of Charlé and Willig.[13]

References

1. M. Pope and C. E. Swenberg, "Electronic Processes in Organic Crystals," Clarendon Press, Oxford 1982.
2. M. Samoc and D. F. Williams, *J. Chem. Phys.*, **78**, 1924 (1983).
3. A. Miniewicz, M. Samoc and D. F. Williams, to be published.
4. M. Samoc, A. Samoc and D. F. Williams, *J. Chem. Phys.*, **76**, 3768 (1982).
5. L. Sebastian, G. Weiser, G. Peter and H. Baessler, *Chem. Phys.*, **75**, 103 (1983).
6. S. Iwata, J. Tanaka and S. Nagakura, *J. Am. Chem. Soc.*, **89**, 2813 (1967).
7. M. Vial and M. Martin-Bouyer, *Mol. Cryst. Liq. Cryst.*, **71**, 219 (1981).
8. M. Samoc, J. B. Webb and D. F. Williams, *Mol. Cryst. Liq. Cryst.*, **62**, 201 (1980).
9. J. Kalinowski and J. Godlewski, *Phys. Stat. Solidi* (*b*), **65**, 789 (1974).
10. H. Killesreiter and H. Baessler, *Chem. Phys. Lett.*, **11**, 411 (1971).
11. G. Vaubel, H. Baessler and D. Mobius, *Chem. Phys. Lett.*, **10**, 334 (1971).
12. H. Baessler, H. Killesreiter and G. Vaubel, *Discuss. Faraday Soc.*, **51**, 48 (1971).
13. K.-P. Charlé and F. Willig, *Chem. Phys. Lett.*, **57**, 253 (1978).
14. D. F. Blossey, *Phys. Rev.*, **B9**, 5183 (1974).
15. R. Haberkorn and M. E. Michel-Beyerle, *Chem. Phys. Lett.*, **23**, 128 (1973).
16. R. G. Enck and G. Pfister in "Photoconductivity and Related Phenomena," ed. J. Mort and D. M. Pai, Elsevier, New York 1976.